Advances in Sciences and Arts
Journal homepage: https://asa.must.ac.mw/

RESEARCH ARTICLE
Vol. 2 Issue 1

Category
Science

3D Density Heterogeneity of the Crust beneath Botswana and its Tectonic Implications

Chikondi Chisenga

Department of Earth Sciences, Malawi University of Science and Technology, P.O. Box 5196, Limbe, Malawi

Correspondence to:
cchisenga@must.ac.mw

Citation
Chisenga (2025). 3D Density Heterogeneity of the Crust beneath Botswana and its Tectonic Implications. *Advances in Sciences and Arts*. 2(1). https://doi.org/10.37872/2025.0102.07

Supporting info
Please refer to the journal's official website on https://asa.must.ac.mw/

Received
10th Sept 2024

Accepted
1st Feb, 2025

Published
14th Mar, 2025

DOI
https://doi.org/10.37872/2025.0102.07

Abstract I present the first information on the 3-D crustal density structure across Botswana obtained from 3D tesseroid inversion of Bouguer anomaly data. Crustal density structure provides important information for understanding tectonic and geodynamic processes in Botswana. I applied the inversion algorithm in spherical coordinates and included constraints consistent with the geological information for Botswana. The results show that density values in Botswana are inhomogeneous, varying from 2650 kg/m^3 to 3000 kg/m^3. Greater variation is noticed in the upper 20 km while the lower crust has a mostly uniform density of ~ 2850 kg/m^3. A combination of density, published Curie point depth, and Moho depth data shows that cratonic regions are mostly characterized by homogenous density values, with presence of mafic intrusions. On the other hand, mobile belts and sedimentary basin exhibit greater density variation, with the presence of > 2800 kg/m^3 density in some of the crustal scale elements. The study further maps possible edges of tectonic terranes. Furthermore, the northern end of Nosop basin indicates possible magnetization in the lower crust, which could be the result of serpentinization.

Keywords: *Remote Sensing, density; Botswana earthquake; crustal structure; inversion; gravity data*

1. Background

Density heterogeneity of the lithosphere can indirectly inform the tectonic structure of the crust, which is paramount to constraining earth's geodynamic processes responsible for density distribution within the crust (Kaban et al., 2018). Thus, it is imperative to determine the resulting heterogeneity of the crust, especially in stable continental regions. In complex tectonic environment, the density variation becomes handy in determining the state of the crust, which points to driving forces in continental tectonic activities.

Botswana is a classic example where the underlying lithosphere comprises the stable continental shield, orogenic mobile belt and incipient rift region. Crustal thickness variation beneath the thick Kalahari sand was unraveled using both seismic observations (e.g., Fadel et al., 2018; Kachingwe et al., 2015; Yu et al., 2015) and gravity observations (Leseane et al., 2015), which showed localized regions of crustal extensions and thinning. However, the crustal variation does not indicate any compositional variation, which could be the effect of either strong or weak mantle density heterogeneity. Furthermore, there is geodetic evidence for a very low strike-slip crustal motion, at a rate about 1 mm/year, in the Okavango Rift Zone (Pastier et al., 2017). Seismological studies also show lower temperature and high velocity in upper mantle in the southern cratonic regions (e.g., James et al., 2001) suggesting a strong lithospheric keel, which could result in basal crustal drag beneath the cratons. Cratonic regions show low temperature, which increases towards the cratonic boundary with orogenic belts (Ballard et al., 1987). These results support a possible low rate of geodynamic processes in the upper crust beneath the stable continental region. However, on April 3, 2017, a dip-slip earthquake of magnitude of M_w 6.5 hit Botswana in the Moiyabana region in the Southern Marginal Zone (SMZ) of the Limpopo-Shashe Belt (Kolawole et al., 2017). Moiyabana region is within a continental stable environment on the cratonic edge of the Kaapvaal Craton. This indicates that the geodynamic state of the crust is not well understood.

In this study, I characterize crustal structure of Botswana to understand the heterogeneity of the crust, as the results of mantle perturbations that indicate the tectonic state of the crust. Seismic studies (e.g., Fadel et al., 2018; Kachingwe et al., 2015; Yu et al., 2015b) provide limited information since they are more sensitive to temperature differences and infer the compositional variations based on seismic velocity (e.g., Tesauro et al., 2014) especially in upper mantle and lower crust. Conversely, gravity data inversely measures crustal density variation, which could give an insight into the compositional variation and heterogeneity of the crust. Nevertheless, it is challenging to give a complete assessment of the lithosphere in such a complex tectonic environment, where different episodes of metamorphism, rifting, accretion and magmatism occurred (Begg et al., 2009; Sippel et al., 2017). Thus, I develop a constrained 3D density model to show the present-day crustal heterogeneity, as a result of mantle heterogeneity and geodynamical processes that indicate crustal deformation.

2. Summary of the tectonic setting of Botswana

Botswana is a relatively flat country located within the southern African tectonic framework, with an estimated area of ~580 730 km^2. The country is entirely covered (~ 80%) by 200 m thick Phanerozoic sediments the Kalahari desert (Haddon, 2005; Fadel et al., 2018), with geological exposure in the eastern region of the country (Key and Ayres, 2000). The tectonic framework of Botswana is made up of two Archean cratons, the Congo Craton to the northwest and the Kalahari Craton (a collage of the Zimbabwe Craton, the Limpopo Mobile Belt and the Kaapvaal Craton) to the southeast separated by the Damara-Ghanzi-Chobe Belt (Figure 1). The current geological understanding is based on the synthesis of geophysics, structural geology and geochemistry, with the latter gleaned from limited outcrops.

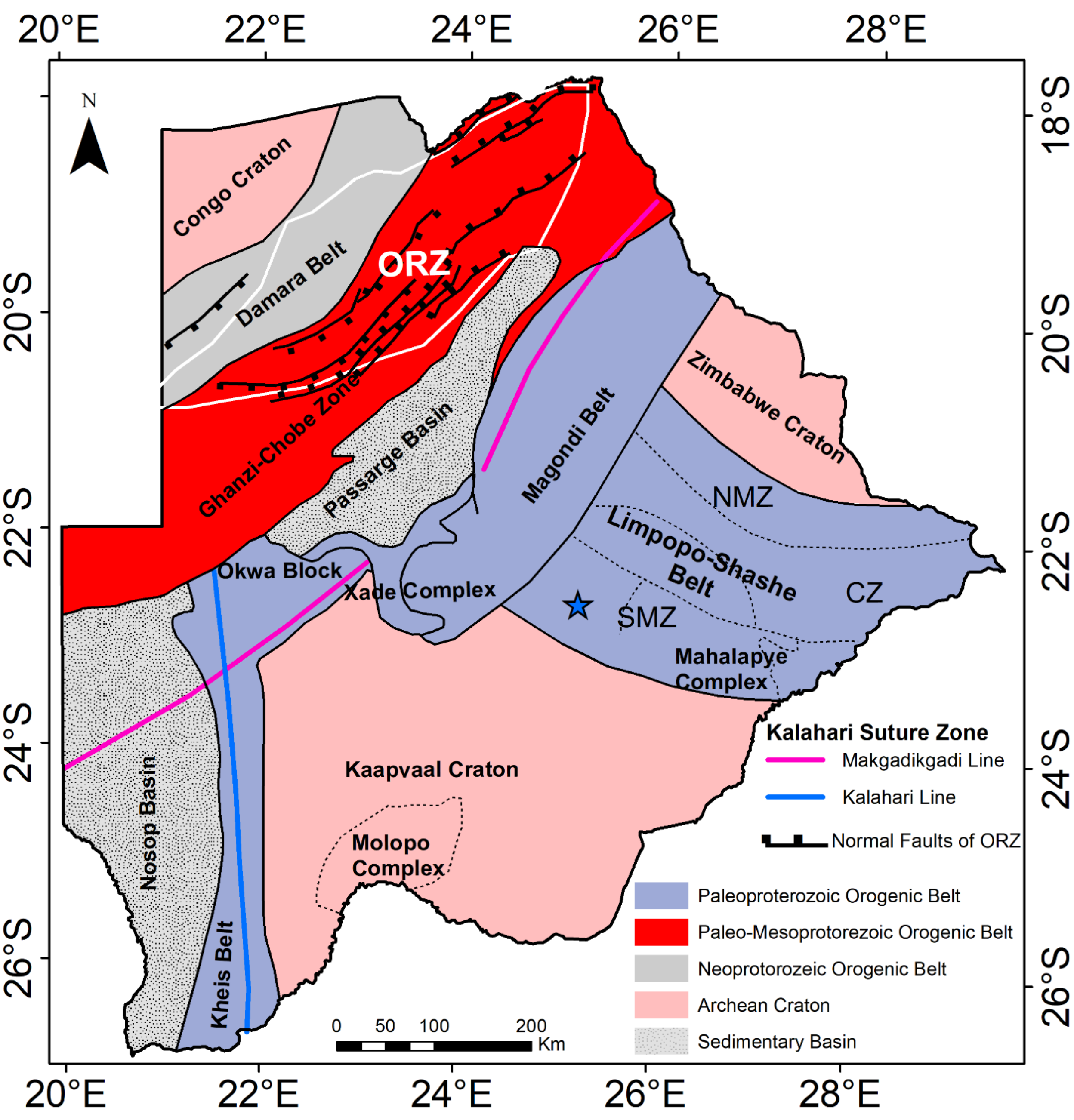

Figure 1: The Precambrian tectonic map of Botswana, modified after Key & Ayres (2000), Ranganai et al. (2002) and Singletary et al. (2003). The white polygon indicates the extent of Okavango Rift Zone after Yu et al., (2015). The blue star shows the location of the M_W 6.5 Botswana earthquake of April 3, 2017

Geochronology and radiometric dating studies suggest that the Kalahari Craton nuclei, of the Kaapvaal Craton and the Zimbabwe Craton, was formed between 3.7 Ga and 2.6 Ga (Begg et al., 2009). The Kaapvaal Craton, which extends from South African into Southern Botswana, is made up of granitoids with gneisses and 3.7-2.7 Ga narrow greenstone belts. The suture between the two nuclei is the 2.7-2.6 Ga high metamorphic grade, NW-SE trending Limpopo-Shashe Belt, which extends into Botswana from eastern Zimbabwe and South Africa (Clifford, 1970). To the northwest, the Limpopo-Shashe Belt is truncated by the NE-SW trending Magondi Belt, the deep Passarge Basin, and Damara-Ghanzi-Chobe Belt. Ranganai et al. (2002) postulated that the boundary between the Limpopo-Shashe Belt boundaries with the Zimbabwe Carton is defined by the Shashe Thrust Zone. Furthermore, he used lithological and structural correlation to subdivide the belt into three marginal zones, the Northern Marginal Zone (NMZ), the Central Zone (CZ), and the Southern Marginal Zone. On the other hand, the southern boundary with the Kaapvaal Craton was placed within the Dinokwe Thrust. The Lechana Fault and the Mahalapye Shear Zone separates the CZ from the SMZ and NMZ.

The northern boundary of the Limpopo-Shashe Belt shows that the belt is truncated by the NE-SW striking Magondi Belt. The relationship is still enigmatic and a subject of debate. The Magondi Belt, which is expressed as low magnetic and gravity response, is concordant with Damara-Ghanzi-Chobe Belt to the north, and their boundary is the Kalahari Suture Zone. The development and evolution of the Damara-Ghanzi-Chobe Belt is closely linked to the collision between the Congo Craton and the Kalahari Craton between 870 and 550 Ma as part of the Damara Orogeny (Begg et al., 2009). The boundary with Congo Craton is still a subject of debate with recent studies placing it within Botswana (e.g., Khoza et al., 2013) while previous studies suggested it was confined within Namibia. The Ghanzi-Chobe Belt is mainly made up of Late Mesoproterozoic to Neoproterozoic northeast and southwestern verging low grade metamorphic sediments. The sediments were deposited on top of the granitoids/gneisses that are preserved on the leading edge of the Congo Craton (e.g., Nguuri et al, 2001; Khoza et al., 2013). The area is suggested to be active due to the overwhelming evidence of classic rift faults with prominent earthquake activity. Most lithospheric studies entail the use of P-wave H-K stacking analysis to understand the lithospheric structures, with findings by Yu et al. (2015) suggesting that there is lack of thinned lithosphere. This observation was echoed by Khoza et al. (2015).

The western boundary of the Kalahari Carton is defined by the 2.0 Ga, north striking Kheis Belt that deflects to the east as the Okwa Belt (James et al., 2001). Locally, the north striking feature consists of Kheis Belt in the southern part and Tshane Complex in the middle part. The Okwa Belt in the north connects to the Xade Complex in central Botswana and the Magondi Belt along the Makgadikgadi line. These belts are characterized by high magnetic crustal features formed along the Kalahari Suture Zone. These features form boundary terranes between the Kaapvaal Craton and the two Proterozoic sedimentary basins, the Passarge Basin located in central Botswana and the Nosop Basin located in western Botswana. The basins contain considerable deposition of

Neoproterozoic and early Paleozoic Ghanzi and Nama sediments, with a maximum depth of ~ 15 km (Key & Ayres, 2000). The thick sediments of Nosop Basin conceal a proposed craton believed to be an extension of the Kalahari Craton (Fadel et al., 2018) or a fragment of an ancient craton called the Maltahohe Craton (Begg et al., 2009).

3. Methodology

3.1 Dataset

The gravity inversion algorithm used the gravity data obtained from the Botswana Geosciences Institute (BGI). The gravity data extended into a rectangular form using Winograd Fourier Transform algorithm (Winograd, 1978, 1979) and then filled with maximum entropy method (Burg, 1975) (Figure 2a). Then, I applied a 1000 km Butterworth high-pass filter to remove mantle contribution(Block et al., 2009), to remain with residual anomaly based on crustal contribution.

I also used crustal thickness data (Chisenga et al., 2019) and Curie Point Depth (CPD) data (Li et al., 2017), which facilitated the tectonic interpretation. The crustal thickness data (Figure 2b) was produced from gravity inversion using the regularized algorithm, which is based on the Gauss-Newton's formulation of Bott's method (Bott, 1960; Silva et al., 2014; Uieda & Barbosa, 2017). The crustal thickness model was then constrained against Botswana's new seismic depth estimates from receiver function and *H-K* stacking analyses (Fadel et al., 2018, Yu et al., 2015, Youssouf et al., 2014). The CPD data (Figure 2c) were obtained from the first global model of Curie-point depth (GCDM) (Li et al., 2017). It is based on the fractal magnetization inversion of magnetic data, which was constrained with many previous regional studies.

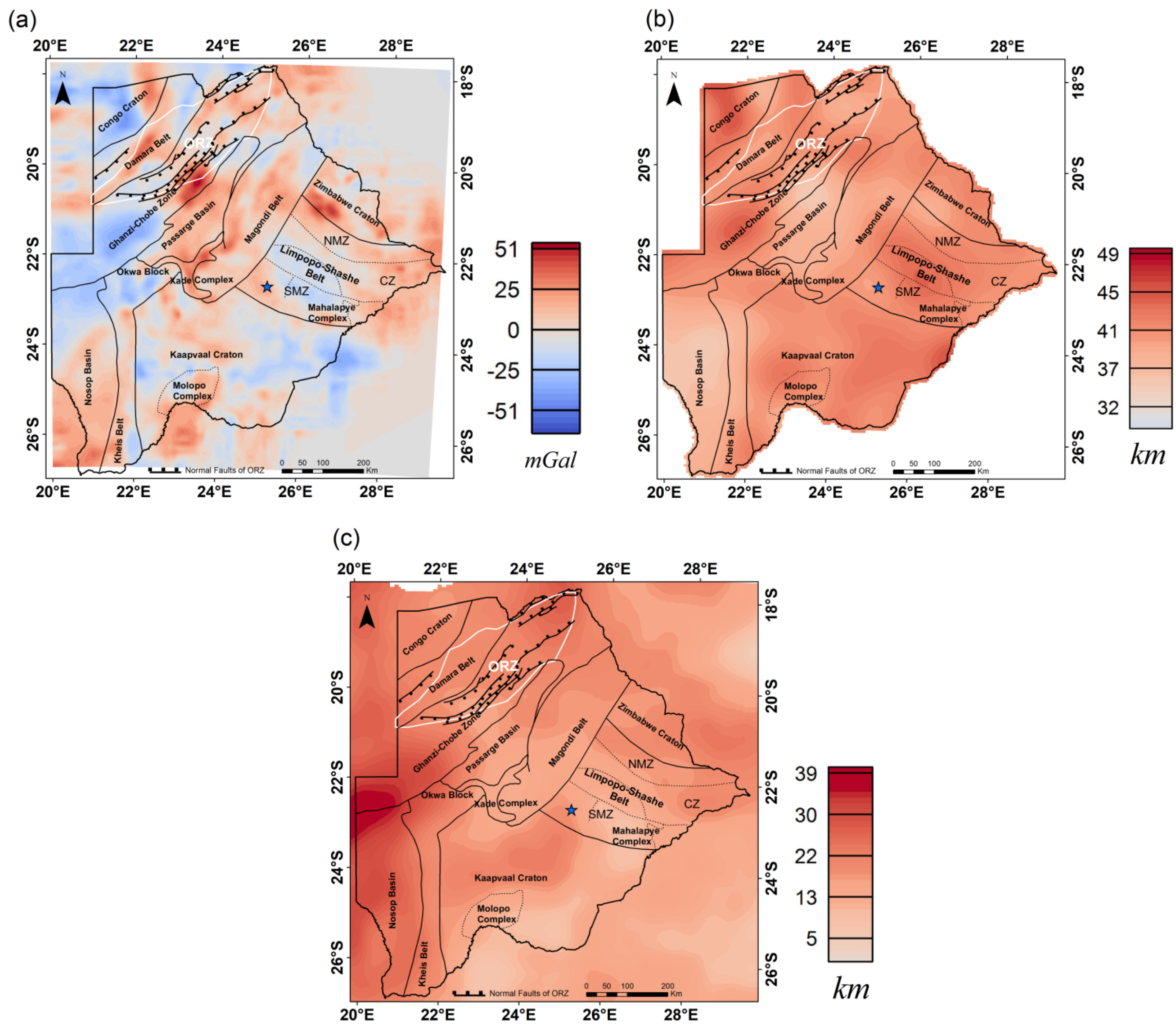

Figure 2: (a) Extended Bouguer anomaly map with a resolution of ~7.5 km; (b) Crustal thickness model (Chisenga et al., 2019); (c) Curie point Depth (CPD) map of Botswana and surrounding areas (Li et al., 2017)

3.2 Density inversion algorithm

The Density inversion applied in this study is based on the depth weighting algorithm (Li and Oldenburg, 1996; 1998), which is formulated as an optimization problem that minimizes the model objective function and the data misfit in the objective function of the density model (Eq. 1). The model objective function is defined as a balance between the physical properties of the reference model and the desired output model. The data misfit is the tradeoff between the calculated data from inverted model and the observed data

$$\phi(m) = \phi_d + \mu\phi_m, \tag{1}$$

where $\phi(m)$ is the objective function, ϕ_d is the data misfit, ϕ_m is the model objective function and μ is the regularization parameter.

The depth weighting function solves the clustering of density values close to surface and counteracts the decay of gravity signal with depth. The algorithm produces a more uniform distribution of density anomalies with depth, which makes it an ideal algorithm for deep density studies. Nevertheless, the depth weighting of Li and Oldenburg (1996; 1998) is implemented in Cartesian Coordinate System (CCS) with uniform prism cells. This limits the algorithm implementation to a small area where the earth curvature can be ignored. For a large area like Botswana, the earth curvature cannot be ignored; since cell size becomes smaller with depth in the radial direction from the surface. Liang et al. (2014) redefined the inversion algorithm in Spherical Coordinate System (SCS) by replacing the rectangular prisms with spherical prisms, called tesseroids. Thus, the cells are rescaled into the same level and the depth weighting function is redefined. The 3D tesseroid inversion was then applied to the residual gravity data with defined optimal parameters to recover a desirable model.

3.3 Implementation

A gravity inversion procedure is an ill-posed problem with non-unique characteristics that produce multiple solutions. We avoided the non-uniqueness of solutions to recover a more realistic density model that satisfies the observed geophysical properties in two ways; by defining the best fit model, and by including geological constraints in the inversion process.

The best fit model was defined as a density model that best describes the model objective function while maintaining the fit with the observed data. This was achieved through the use of an optimal regularization parameter (Tikhonov and Arsenin, 1977) in the objective parameter (Eq. 1). A regularization parameter is a trade-off between the model objective function and data misfit. I iteratively searched for the optimal regularization parameter that is defined in the objective function of the Li and Oldenburg (1996, 1998) algorithm. I invented the gravity data with 13 different values of regularization parameter (Figure 3). The resulting model objective function was plotted against the data misfit for each of the regularizing parameter. The resulting plot, called the L-curve method (Lawson and Hanson, 1974), indicates the optimal value of regularization parameter as a value that lies at the corner of the L-curve. As shown in Figure 3, the optimal regularization parameter value was 2.5, which best fits the data while producing a desirable density model.

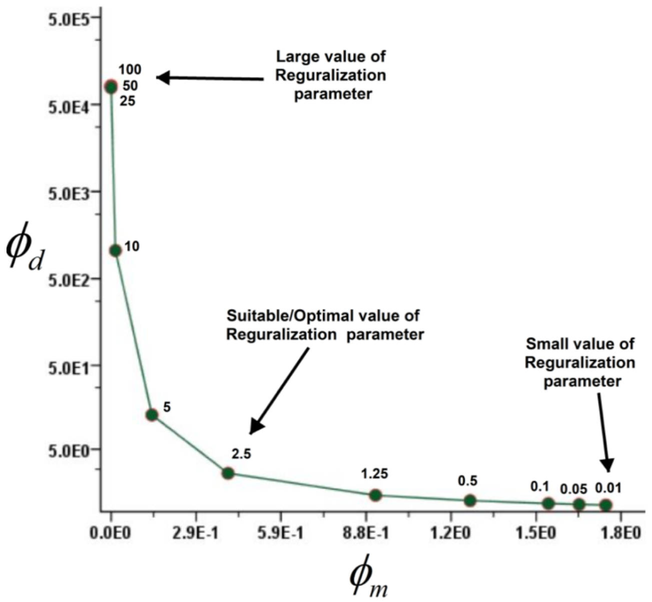

Figure 3: L-curve solution for data misfit (ϕ_d) against model objective function (ϕ_m).

The inversion algorithm also includes a penalty factor and geological/geophysical constraint during inversion using the Lagrangian multiplier (Rockafellar, 1970). The penalty factor makes the recovered model more reliable while the geological constraints improve the inversion results (Zhang et al., 2018). The approach constrains the inversion results within a defined range while obeying other inversion criteria. The penalty factor is assigned as a small value of 1.0×10^{-6} (with an increment of 2) and iteratively increased until the penalty factor fits the constraints information (Zhang et al., 2015). The geological upper and lower density constrains are based on the crustal densities, relative to the average crustal density value. Normally, continental crust has density variation between 2650 kg/m^3 and 2950 kg/m^3 with an average of 2800 kg/m^3. Due to occurrences of two sedimentary basins (Haddon, 2005), I extend the lower bound to 2450 kg/m^3. Nevertheless, Botswana is known to have mafic complexes in the crust (Hutchins and Reeves, 1980; Key and Ayres, 2000), which have assumed grain density of 3200 kg/m^3. Therefore, the density contrast in our inversion is allowed to vary between -350 kg/m^3 and 400 kg/m^3, relative to the assumed continental mean density value of 2800 kg/m^3.

I then prepared the 3D mesh and input dataset for inversion as illustrated in Table 1. I set the reference radius to the mean radius of the earth of 6173 km. The background density was set to zero (0) kg/m^3 to obtain density contrast values, considering that this value represents the average crustal density value of 2800 kg/m^3 in absolute density terms. The depth extent of the inversion was set to 50 km, since the deepest point on the Moho obtained from seismic studies in Botswana is 50 km in the western Zimbabwe Craton (Fadel et al., 2018). Finally, the density perturbation solutions from the applied constrained 3D tesseroid inversion were resolved using Eq. 2 as defined by Zhang et al. (2015).

$$\left[G^TW_d^TW_dG+\mu W_m^TW_m+\frac{1}{2}M(F_1+F_2+F_3)\right]m=G^TW_d^TW_dd^{obs}+\mu W_m^TW_mm_{ref}-F_0\lambda_0^T+F_1\lambda_1^T-F_2\lambda_2^T+\frac{1}{2}M(F_0m_0+F_1m_1+F_2m_2)+\frac{1}{2}M(F_1z_1^2-F_2z_2^2)$$

(2)

where the diagonal of the matrix F_i denotes the index of the constrained information in each divided rectanglular cell, d^{obs} is observed data; G is the kernel function, which denotes the relationship between the geological model and the observed data; W_d is the weighting matrix for data misfit; W_m is weighting matrix for the model objective function, μ is the regularization parameter, M is the penalty factor, λ represents Lagrangian multipliers and z_i is the slack variable of the *i*th cell, where *i* is the index number for each cell.

Table 1: The 3D mesh and dataset for inversion

Region	Inversion range	Model		Data	
		Grid size	Grid number	Data size	Data number
	Longitude	0.1°	112	0.1°	112
	Latitude	0.1°	112	0.1°	112
Botswana	Depth	0 – 50 km		0 – 50 km	
	Radial direction	2 km	17	2 km	17

4. Results and Discussion

The density structure beneath Botswana shows crustal density variability ranges from 2650 kg/m^3 to 3000 kg/m^3. The variability differs in tectonic terranes; lower values are noticed in sedimentary basins and mobile belts and higher values in cratonic areas and mafic complexes. I identified subsurface structures from the existence of density structures from the surface to a depth of 50 km. The variability is mostly noticed in the first 20 km and the lower crust seems to have a uniform density, around the 2800 kg/m^3 mean value. The results are shown as horizontal depth slices and vertical cross-sections (Figures 4, 5 and 6) of the obtained density models. Density structures for different tectonic terranes based on terrain age and their tectonic implications are presented and discussed in subsequent subsection.

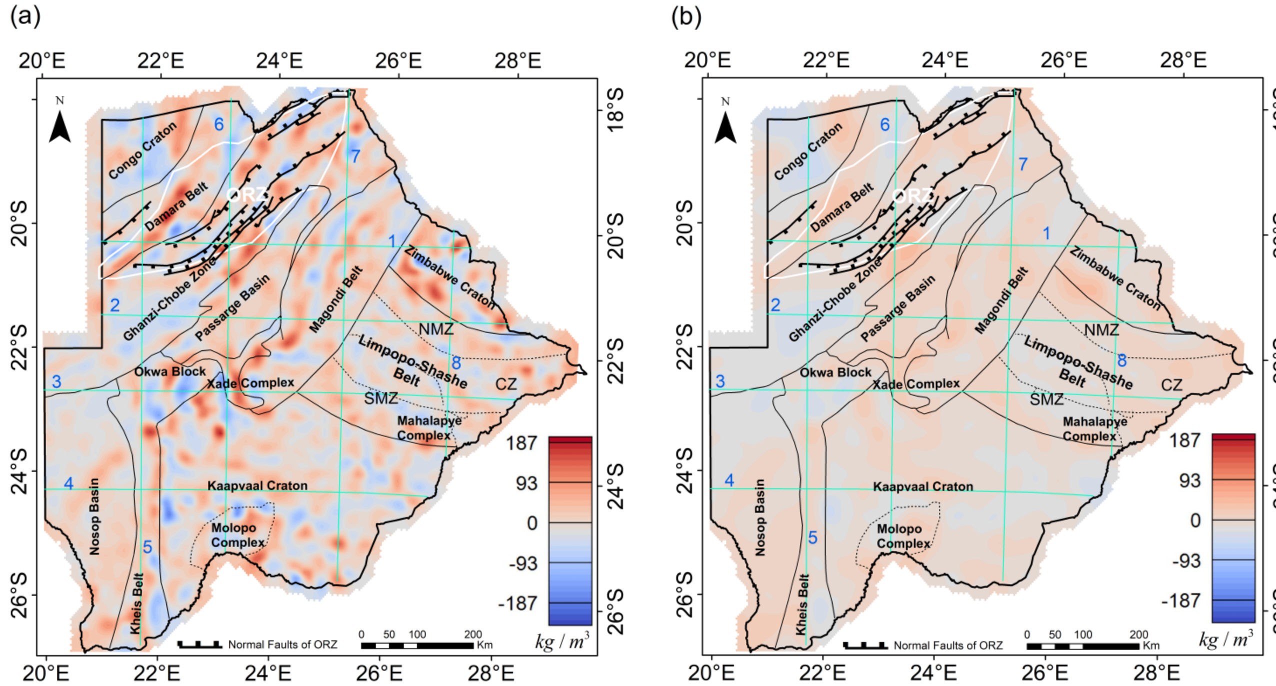

Figure 4: Horizontal slices of the subsurface density structures: (a) at the depth of 20 km; and (b) at the depth of 40 km. The cyan lines indicate the location of profiles for the vertical cross sections as presented in Figures 5 and 6.

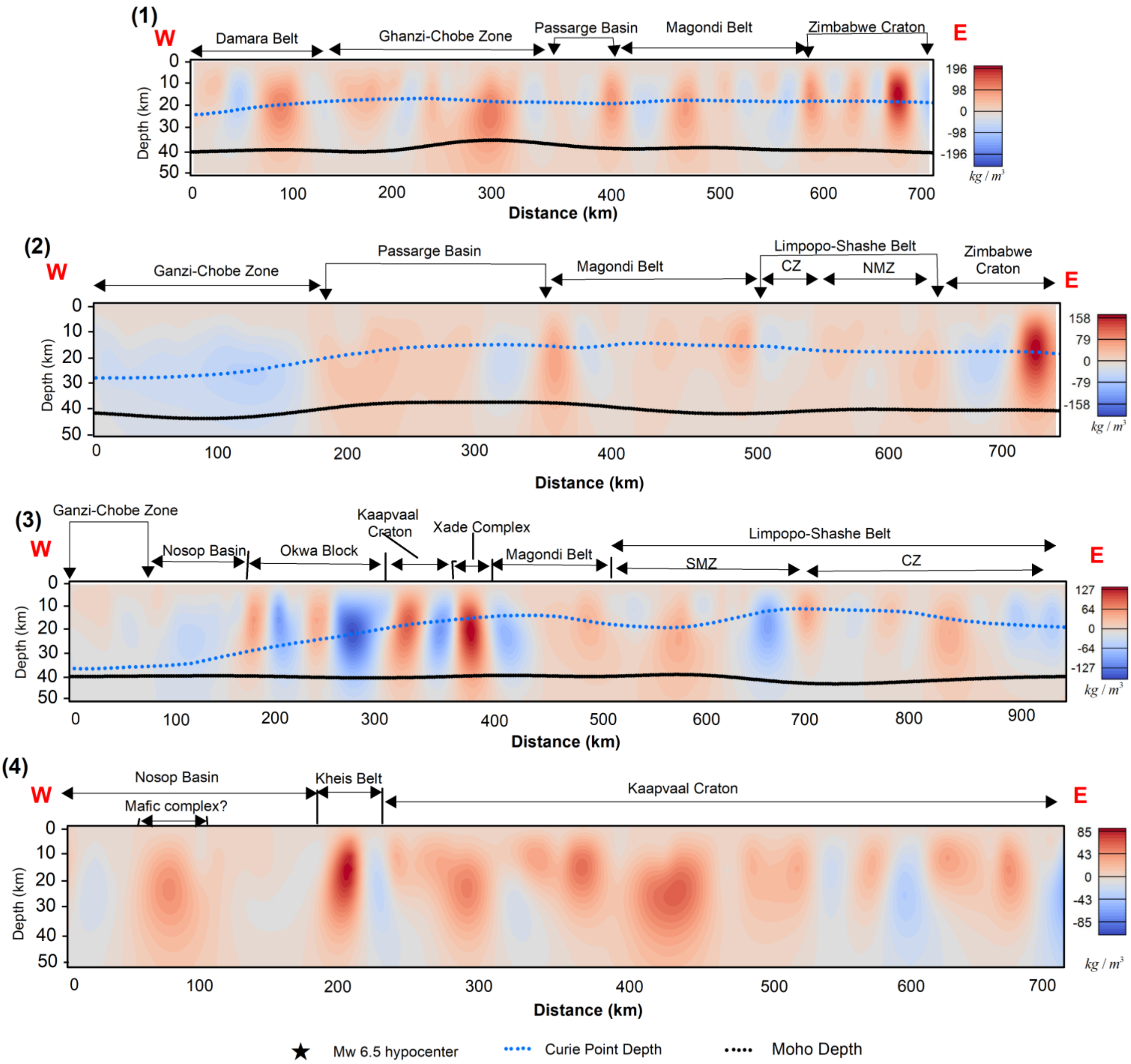

Figure 5: The E-W orientated vertical cross-sections of the 4 profiles as shown on Figure 4 for lines 1, 2, 3 and 4. The blue dotted line represents the Curie Point Depth after Li et al. (2017) and Black line represents the Moho depth after Chisenga et al. (2019). The vertical axis was exaggerated by a factor of 2.

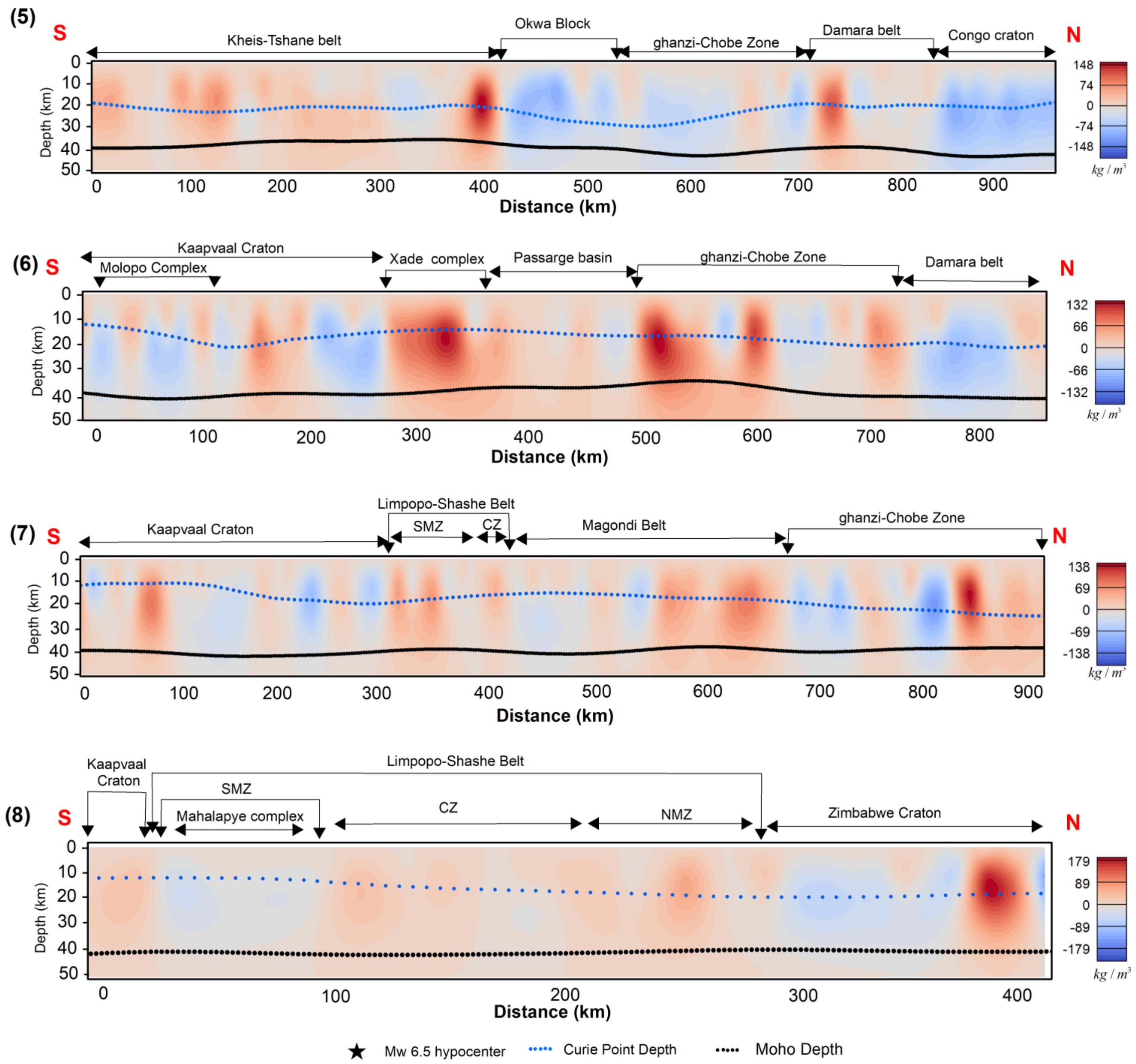

Figure 6: The N-S orientated vertical cross-sections of the 4 profiles as shown on Figure 4 for lines 5, 6, 7 and 8. The blue dotted line represents the Curie Point Depth after Li et al. (2017) and Black line represents the Moho depth after Chisenga et al. (2019). The vertical axis was exaggerated by a factor of 2, excerpt for line 8.

4.1 Archean crust

The crustal density structure of the Kaapvaal Craton is mostly inhomogeneous and varies between 2650 kg/m^3 to 2950 kg/m^3. The craton also shows a variation in thickness from 39 km to 46 km (Chisenga et al., 2019) with shallow CPD (Li et al., 2017). The most profound feature is the clear boundary with surrounding tectonic terranes, e.g.

the Kheis Belt (Profile 4 on Figure 5), the Xade Complex (Profile 5 on Figure 6) and the Limpopo-Shashe Belt (Profile 7 on Figure 6). This suggests that the boundary of the craton, which was illusive, can be determined to some extent based on the lithological and density variation. High-density structures are noticed correlating with known Proterozoic mafic complexes that intruded the craton, e.g. Molopo Farm Complex and Tsetseng Complex. The mafic complexes are completely covered by the Kalahari Group and are characterized by density values > 2900 kg/m^3. The craton also shows an intermediate to mafic lower crust with density values around 2850 kg/m^3, which corroborates with the Vp/Vs values of 1.74–1.82 (Fadel et al., 2018). The Molopo Farm Complex in southern Botswana shows higher values larger than 2950 kg/m^3 at a depth of 20 km (Figure 4a). This could suggest that the mafic intracratonic Bushveld complex intrusion of South Africa extended into Botswana (Nair et al., 2006; Fadel et al., 2018), as most complexes in this region show high gravity and magnetic values (Ramotoroko et al., 2016).

Western Zimbabwe Craton shows relatively lower density values < 2900 kg/m^3 compared to values of the Kaapvaal Craton. Most notably anomalous is the high-density intrusion located at the depth of ~10 km with density values of ~3000 kg/m^3, as seen in both vertical cross-section (Figures 5 and 6) which extend to the depth of 20 km as it is visible on the horizontal slice (Figure 4). The craton shows an average crustal thickness of 41 km with CPD of ~ 12 km. The thinner crust in the Zimbabwe Craton, ~40 km (Chisenga et al., 2019) that was estimated to be ~50 km from seismic studies (e.g., Fadel et al., 2018; Youssof et al., 2013) shows a lower crust density value of ~2800 kg/m^3. This suggests an intermediate composition, which is slightly different to a felsic lower crust with a V_p/V_s of 1.69 - 1.75 based on seismic studies (Fadel et al., 2018). The area shows a low density, ~ 2700 kg/m^3, surrounded by high-density lithology as seen at the depth of 20 km (Figure 4). This could be a result of the crustal reworking and fractionated magma chamber that led to the placement of the Karoo Dyke Swarms. The region is shown to have a shallow CPD of ~ 15 km (Li et al., 2017) with elevated heat flow (Ballard et al., 1987).

The density value of the Congo Craton is homogenously consisting of density values of < 2800 kg/m^3. However, there are some regions that show high-density values of > 2800 kg/m^3. The spatial extent of the Congo Craton (Khoza et al., 2013; Yu et al., 2015b; Fadel et al., 2018; Chisenga et al., 2019) is interpreted as a Proterozoic crust with the following terranes ; Quangwadum Complex, Tsidilo Hill Group, and Xaudum Group (Key and Ayres, 2000). Chisenga et al. (2019) suggested an over-thrust collisional zone in which the Proterozoic crust lies on top of the Congo Craton. The region has a lower crustal density value of 2700 kg/m^3, which was also proposed to be a felsic composition of a reworked crust, similar to cratons (Fadel et al., 2018). The region with 2700 kg/m^3 could represent granitic composition. This is not surprising as few outcrops in the area (Key and Ayres, 2000) suggest a buried syenite, granite, granitic gneiss and gnessetic granitoid of Quangwadum complex.

4.2 Neo-Archean Mobile Belt

The Limpopo-Shashe Belt forms a relatively inhomogeneous density terrane for the three sub-terranes of the SMZ, the CZ and the NMZ. The boundary of the Limpopo-Shashe Belt between the Kaapvaal and the Zimbabwe Cratons has already been mapped using gravity data (Ranganai et al., 2002). The SMZ shows density values of less than 2800 kg/m^3. The thinnest crust, of ~ 40 km, in the Limpopo-Shashe Belt is in the SMZ, which corresponds to the April 3, 2017 Botswana earthquake along the boundary with the Kaapvaal Craton. The region shows lower density values of ~ 2750 kg/m^3 on the epicentral region for the earthquake (Figure 7). The CZ is characterized by density values of 2700 kg/m^3, shallow CPD of ~ 10 km and a thick crustal thickness of 46 km (Profile 3 on Figure 5). Heat flow is elevated in the region, ~ 60 mW m^{-2} (Ballard et al., 1987). This region has a pop-up structure with thick lithosphere, which was interpreted to be a collisional zone between the Kaapvaal Craton and the Zimbabwe Craton (Ranganai et al., 2002; Roering et al., 1992; Fadel et al., 2018). The NMZ has a flat crust south of the Moiyabana region relative to the surrounding Zimbabwe Craton (Chisenga et al., 2019), which signifies little deformation. This is also visible in the density structure, with almost uniform density values of around 2800 kg/m^3.

4.3 Proterozoic Mobile Belts

The Ghanzi-Chobe Zone constitutes two crustal density divisions. The southwestern division exhibits low density values of < 2800 kg/m^3. This region has a felsic lower crust (Profile 2 on Figure 5), which is slightly different from the intermediate lower crust from seismic information with V_p/V_s of 1.81 (Fadel et al., 2018). It also has a thick crust of 46 km (Chisenga et al., 2019), which possibly represents evidence/remnants of a collisional zone for the Congo Craton and the Kalahari Craton. The region has the deepest CPDs that range from 28 km (Profile 2 on Figure 5) to 39 km (Profile 3 on Figure 5). The location of Curie point in the lower crust close to the Moho could signify magnetization of the lower crust. Li et al. (2013) suggested that the magnetic source in upper mantle or lower crust could be the result of serpentinization. The northeastern division of the Ghanzi-Chobe Zone is related to ORZ extension. The region shows high-density values of > 2800 kg/m^3. The ORZ and the surrounding region show a mafic lower crust of > 2900 kg/m^3, a thin crust of ~ 37 km and CPD of ~ 20 km (Profile 1 on Figure 5), which is similar to the mafic lower crust with V_p/V_s of 1.88 (Fadel et al., 2018). Furthermore, the region contains considerable high-density rocks of ~ 3000 kg/m^3 (Profile 1 on Figure 5). This suggests the presence of mafic rocks beneath the Kalahari cover in the ORZ. The fault geometry aligns with the recovered density at the depth of 20 km, in which low density rocks are within the rifting zone and high-density are outside the fault system (Figure 4a). They show a NW-SE extension. The region, however, shows shallow CPD and Moho depth (Profile 1 on Figure

5; Leseane et al., 2015), which suggest that the mafic bodies are not magnetized. It could also mean that the mafic bodies exhibit little influence of the bimodal basaltic volcanic that formed the Kgwebe Formation around ~ 1106 Ma during the initiation of the Northwest Botswana rift (Carney et al., 1994; Modie, 1996).

The Damara Belt was formed due to the collision of the Congo Craton and the Kalahari Craton during the Pan-African and Damara orogeny (Gray et al., 2008). It is in the south-eastern side of the Congo Craton. The density structure of this belt consists of two NE-SW striking features (Figure 2a). The first is the kidney-shaped feature with density values > 2900 kg/m^3 (Figure 4), locally called Roibok Complex with granite gneiss and to some extent amphibolite (Key and Ayres, 2000; Singletary et al., 2003). It shows a thick crust of ~40 km with average heat flow as evidenced by shallow CPD at ~ 18 km. Horizontal density slice at the depth of 20 km indicates two different lithologies, the NE-SW and N-S striking features (Figure 4). The other region, locally called the Kwando Complex, is located east of the Roibok Complex, which has a northeasterly striking magnetic body of Granite gneiss, granite, amphibole-gneiss, migmatite and meta dolerite (Carney et al., 1994). Profile 6 on Figure 6 shows a low- density body of ~ 2700 kg/m^3, which also fits the geology of the area as granitic crustal block with a felsic lower crust.

The Paleoprotorezoic Magondi-Xade-Okwa-Kheis-Tshane Belts were formed during the Eburnean Orogeny (Begg et al., 2009) along the KSZ. The Kheis Belt and the Tshane Complex are north-south oriented features along the Kalahari Line, with thin crust and relatively deep CPD. The highest density values are in the Tshane Complex of ~ 2950 kg/m^3, possibly due to the unexposed basic-ultrabasic rock bodies (Carney et al., 1994; Key and Ayres, 2000). The Kheis Belt shows a relatively lower density of ~2850 kg/m^3 along the boundary with the Kaapvaal Craton. The Okwa Block in northern end of the Kheis-Tshane Belt show lower density values of 2700 kg/m^3 (Profile 5 of Figure 6). The low density region of the Okwa Block shows bulged Paleoprotorezoic crusts, which interpreted to represent a post-Archean reworking during the Eburnean Orogeny (Fadel et al., 2018; Chisenga et al., 2019). Nevertheless, the CPD is deeper in the Okwa Complex than the Kheis-Tshane Belt. The Xade Complex shows high-density values of 2900 kg/m^3 with an intermediate lower crust. Magondi Belt has a flat crust in the middle that thickens toward the Limpopo-Shashe Belt (Chisenga et al., 2019).

4.4 Sedimentary Basins

The Nosop Basin has density values of ~ 2750 kg/m^3 in the northern part, and around 2800 kg/m^3 in the southern part. The Nosop Basin has an accumulation of Ghanzi and Nama group sediment thickness of ~15 km (Key and Ayres, 2000). Nevertheless, the crust is thin at ~ 38 km (Fadel et al. 2018; Chisenga et al., 2019), which suggests basement thickness of ~24 km. The northern Nosop shows a deep CPD of ~37 km within a region with a crust thickness of ~39 km (Profile 3 on Figure 5). As already discussed, this could suggest serpentinization of the upper mantle and in some cases lower crust (Li et al., 2013). Serpentinization in the upper mantle creates a low velocity zone (e.g., Mevel, 2003), which was also noticed in this region from seismic data (Fadel et al., 2018). It also shows a lower intermediate crust with density values of ~ 2700 kg/m^3. The central Nosop Basin shows ~ 2850 kg/m^3 density value region beneath the 15 km thick sediments in mid-crust at the depth of ~ 20 km (Figure 4a). Conversely, the Passarge Basin show relatively higher density values with an average of ~ 2850 kg/m^3, despite similar crustal thickness as the Nosop Basin. The crust is however thinner, at ~ 37 km, but unlike the Nosop, it shows a shallower CPD of ~25 km. The Basin also shows an intermediate to mafic lower crust (Profile 2 on Figure 5), like seismic derived lower crust composition (Fadel et al., 2018).

5. Conclusion

We have provided the first information on the vertical and horizontal density variation in Botswana. We used the 3D tesseroid inversion algorithm that considered the earth curvature and geophysical constraints to provide the insight into the crustal density structure beneath Botswana from gravity data. The results show that density structure of Botswana is inhomogeneous, varying from 2650 kg/m^3 to 3000 kg/m^3. It is mostly dependent on the tectonic terrane age with greater variation noticed in Proterozoic mobile belts than in Archean terranes. Generally, the upper 20 km of the crust accounts for the variation that is noticed while the lower crust has a mostly uniform density of ~ 2850 kg/m^3. Together with previous studies of Curie point depth and Moho depth data, we suggested that the northern end of Nosop basin could be magnetized in the lower crust from the introduction of serpentinization.

Acknowledgement

We thank the Botswana Geoscience Institute (BGI), formerly the Geological Survey of Botswana, for providing the gravity data.

Reference

Ballard, S., Pollack, H.N., Skinner, N.J., 1987. Terrestrial Heat-Flow in Botswana and Namibia. J. Geophys. Res. Earth Planets 92, 6291–6300. https://doi.org/10.1029/JB092iB07p06291

Begg, G.C., Griffin, W.L., Natapov, L.M., O'Reilly, S.Y., Grand, S.P., O'Neill, C.J., Hronsky, J.M.A., Djomani, Y.P., Swain, C.J., Deen, T., Bowden, P., 2009. The lithospheric architecture of Africa: Seismic tomography, mantle petrology, and tectonic evolution. Geosphere 5, 23–50. https://doi.org/10.1130/GES00179.1

Block, A.E., Bell, R.E., Studinger, M., 2009. Antarctic crustal thickness from satellite gravity: Implications for the Transantarctic and Gamburtsev Subglacial Mountains. Earth Planet. Sci. Lett. 288, 194–203. https://doi.org/10.1016/j.epsl.2009.09.022

Bott, M.H.P., 1960. The use of rapid digital computing methods for direct gravity interpretation of sedimentary basins. Geophys. J. Int. 3, 63–67.

Burg, J.P., 1975. Maximum entropy spectral analysis. Unpublish Ph.D Thesis, Staford university.

Carney, J.N., Aldiss, D.T., Lock, N.., 1994. The geology of Botswana. Bulletin 37,Botswana Geological Survey Department (currently Botswana Geoscience Institute)

Chisenga, C., Meijde, M. Van der, Jianguo, Y., Atekwana, E.A., Fadel, I., 2019. Gravity derived crustal thickness map of Botswana: Implication to the Mw 6.5 April 3, 2017 Botswana earthquake. in review. Tectonophysics.

Clifford, T.N., 1970. The structural framework of Africa, in: Clifford, T.N., Gass, I.G. (Eds.), African Magmatism and Tectonics. Oliver and Boyd, Edinburgh, pp. 1–26.

Fadel, I., Meijde, M. Van Der, Paulssen, H., 2018. Crustal Structure and Dynamics of Botswana. J. Geophys. Res. Solid Earth. https://doi.org/10.1029/2018JB016190

Gray, D.R., Foster, D., Meert, J., Goscombe, B., Armstrong, B., Trouw, R., Passchier, C., 2008. A Damara orogen perspective on the assembly of south- western Gondwana. Geol. Soc. London, Spec. Publ. 294, 257–278.

Haddon, I.G., 2005. The Sub-Kalahari Geology and Tectonic Evolution of the Kalahari Basin, Southern Africa. Thesis. University of Witswatesland.

Hutchins, D.G., Reeves, C.V., 1980. Regional geophysical exploration of the Kalahari in Botswana. Tectonophysics 69, 201–220. https://doi.org/10.1016/0040-1951(80)90211-5

James, D.E., Fouch, M.J., VanDecar, J.C., van der Lee, S., Kaapvaal Seismic Group, 2001. Tectospheric structure beneath southern Africa. Geophys. Res. Lett. 28, 2485–2488. https://doi.org/10.1029/2000GL012578

Kaban, M.K., Khrepy, S. El, Al-arifi, N., 2018. Density structure and isostasy of the lithosphere in Egypt and their relation to seismicity. Solid Earth 9, 833–846.

Kachingwe, M., Nyblade, A., Julià, J., 2015. Crustal structure of Precambrian terranes in the southern African subcontinent with implications for secular variation in crustal genesis. Geophys. J. Int. 202, 533–547. https://doi.org/10.1093/gji/ggv136

Key, R.M., Ayres, N., 2000. The 1998 edition of the National Geological Map of Botswana. J. African Earth Sci. 30, 427–451. https://doi.org/10.1016/S0899-5362(00)00030-0

Khoza, T.D., Jones, A.G., Muller, M.R., Evans, R.L., Miensopust, M.P., Webb, S.J., 2013. Lithospheric structure of an Archean craton and adjacent mobile belt revealed from 2-D and 3-D inversion of magnetotelluric data : Example from southern Congo craton in northern Namibia. J. Geophys. Res. 118, 4378–4397. https://doi.org/10.1002/jgrb.50258

Kolawole, F., Atekwana, E.A., Malloy, S., Stamps, D.S., Grandin, R., Abdelsalam, M.G., Leseane, K., Shemang, E.M., 2017. Aeromagnetic, gravity, and Differential Interferometric Synthetic Aperture Radar analyses reveal the causative fault of the 3 April 2017 Mw 6.5 Moiyabana, Botswana, earthquake. Geophys. Res. Lett. 44, 8837–8846. https://doi.org/10.1002/2017GL074620

Lawson, C.L., Hanson, R.J., 1974. Solving Least Squares Problem. Prentice-Hall, New Jersey.

Leseane, K., Atekwana, E.A., Mickus, K.L., Abdelsalam, M.G., Shemang, E.M., Atekwana, E.A., 2015. Thermal perturbations beneath the incipient Okavango Rift Zone, northern Botswana. J. Geophys. Res. Solid Earth 120, 1210–1228. https://doi.org/10.1002/2014JB011029

Li, C., Lu, Y., Wang, J., 2017. A global reference model of Curie- point depths based on EMAG2. Sci. Rep. 1–9. https://doi.org/10.1038/srep45129

Li, C.F., Wang, J., Lin, J., Wang, T., 2013. Thermal evolution ofthe North Atlantic lithosphere: new constraints from magnetic anomaly inversion with a fractal magnetization model. Geochemistry, Geophys. Geosystems 14, 5078–5105.

Li, Y., Oldenburg, D.., 1998. 3-D inversion of gravity data. Geophysics 63, 264–267.

Li, Y., Oldenburg, D.W., 1996. 3-D inversion of magnetic data. Geophysics 61, 394–408.

Liang, Q., Chen, C., Li, Y., 2014. 3-D inversion ofgravitydata in spherical coordinates with application to the GRAIL data. J. Geophys. Res. Planets Res. 119, 1359–1373. https://doi.org/10.1002/2014JE004626.Received

Mevel, C., 2003. Serpentinization of abyssal peridotites at mid-ocean ridges. Comptes Rendus Geosci. 335, 825–852.

https://doi.org/htto://doi.org/10.1016/j.crte.2003.08.006

Modie, B.N.J., 1996. Depositional environments of the Meso- to Neoproterozoic Ghanzi-Chobe belt, northwest Botswana. J. African Earth Sci. 22, 255–268. https://doi.org/10.1016/0899-5362(96)00014-0

Nair, S.K., Gao, S.S., Liu, K.H., Silver, P.G., 2006. Southern African crustal evolution and composition: Constraints from receiver function studies. J. Geophys. Res. Earth 111. https://doi.org/https://doi.org/10.1029/2005JB003802

Pastier, A.M., Dauteuil, O., Murray-Hudson, M., Moreau, F., Walpersdorf, A., Makati, K., 2017. Is the Okavango Delta the terminus of the East African Rift System? Towards a new geodynamic model: Geodetic study and geophysical review. Tectonophysics 712–713, 469–481. https://doi.org/10.1016/j.tecto.2017.05.035

Ramotoroko, C.D., Ranganai, R.T., Nyabeze, P., 2016. Extension of the Archaean Madibe-Kraaipan granite-greenstone terrane in southeast Botswana: Constraints from gravity and magnetic data. J. African Earth Sci. 123, 39–56. https://doi.org/10.1016/j.jafrearsci.2016.06.016

Ranganai, R.T., Kampunzu, A.B., Atekwana, E.A., Paya, B.K., King, J.G., Koosimile, D.I., Stettler, E.H., 2002. Gravity evidence for a larger Limpopo Belt in southern Africa and geodynamic implications. Geophys. J. Int. 149. https://doi.org/10.1046/j.1365-246X.2002.01703.x

Rockafellar, R.T., 1970. Convex Analysis. Princeton University Press, New Jersey.

Roering, C., Reenen, D.D. Van, Smit, C.A., Jr, J.M.B., Beer, J.H. De, Wit, M.J. De, 1992. Tectonic model for the evolution of the Limpopo Belt. Precambrian Res. 55, 539–552. https://doi.org/https://doi.org/10.1016/0301-9268(92)90044-O

Silva, J., Santos, D., Gomes, K., 2014. Fast gravity inversion of basement relief. Geophysics 79, G79–G91.

Singletary, S.J., Hanson, R.E., Martin, M.W., Crowley, J.L., Bowring, S.A., Key, R.M., Ramokate, L. V., Direng, B.B., Krol, M.A., 2003. Geochronology of basement rocks in the Kalahari Desert, Botswana, and implications for regional Proterozoic tectonics. Precambrian Res. 121, 47–71. https://doi.org/10.1016/S0301-9268(02)00201-2

Sippel, J., Meeßen, C., Cacace, M., Mechie, J., Fishwick, S., Heine, C., Scheck-wenderoth, M., Strecker, M.R., 2017. The Kenya rift revisited : insights into lithospheric strength through data-driven 3-D gravity and thermal modelling. Solid Earth 8, 45–81.

https://doi.org/10.5194/se-8-45-2017

Tesauro, M., Kaban, M.K., Mooney, W.D., Cloetingh, S., 2014. Density, temperature, and composition of the North American litho- sphere – New insights from a joint analysis of seismic, gravity, and mineral physics data: 2. Thermal and compositional model of the upper mantle. Geochemistry, Geophys. Geosystems G3, 4808–4830. https://doi.org/https://doi.org/10.1002/2014GC005484,

Tikhonov, A.N., Arsenin, V.Y., 1977. Solutions of Ill-Posed Problems. Winston and Sons, Washington DC.

Uieda, L., Barbosa, V.C.F., 2017. Fast nonlinear gravity inversion in spherical coordinates with application to the South AmericanMoho. Geophys. J. Int. 208, 162–176. https://doi.org/10.1093/gji/ggw390

Winograd., S., 1979. On the multiplicative complexity of the Discrete Fourier Transform. Adv. Math. (N. Y). 32, 83–117. https://doi.org/http://doi.ord/10.1016/0001-8708(79)90037-9

Winograd., S., 1978. On Computing the Discrete Fourier Transform. Math. Comput. 32, 175–199.

Youssof, M., Thybo, H., Artemieva, I.M., Levander, A., 2013. Moho depth and crustal composition in Southern Africa. Tectonophysics 609, 267–287. https://doi.org/10.1016/j.tecto.2013.09.001

Yu, Y., Liu, K., Moidaki, M., Mickus, K., Atekwana, E.A., Gao, S.S., 2015a. A joint receiver function and gravity study of crustal structure beneath the incipient Okavango Rift, Botswana. Geophys. Res. Lett. 42, 8398–8405.

Yu, Y., Liu, K.H., Moidaki, M., Reed, C.A., Gao, S.S., 2015b. No thermal anomalies in the mantle transition zone beneath an incipient continental rift: Evidence from the first receiver function study across the Okavango Rift Zone, Botswana. Geophys. J. Int. 202, 1407–1418. https://doi.org/10.1093/gji/ggv229

Zhang, Y., Wu, Y., Yan, J., Wang, H., Rodriguez, J.A.P., Qiu, Y., 2018. 3D inversion of full gravity gradient tensor data in spherical coordinate system using local north - oriented frame. Earth, Planets Sp. 70. https://doi.org/10.1186/s40623-018-0825-5

Zhang, Y., Yan, J., Li, F., Chen, C., Mei, B., Jin, S., Dohm, J.H., 2015. A new bound constraints method for 3-D potential field data inversion using Lagrangian multipliers. Geophys. J. Int. 201, 267–275. https://doi.org/10.1093/gji/ggv016